Spectrochimica Acta Part A 78 (2011) 763–770

Contents lists available at ScienceDirect

Spectrochimica Acta Part A: Molecular and Biomolecular Spectroscopy

journal homepage: www.elsevier.com/locate/saa

Synthesis, characterization, antibacterial activity, SOD mimic and interaction with DNA of drug based copper(II) complexes

Mohan N. Patel[a,*], Promise A. Dosi[a], Bhupesh S. Bhatt[a], Vasudev R. Thakkar[b]

[a] Department of Chemistry, Sardar Patel University, Vallabh Vidyanagar 388 120, Gujarat, India
[b] BRD School of Bioscience, Sardar Patel University, Vallabh Vidyanagar 388 120, Gujarat, India

ARTICLE INFO

Article history:
Received 14 July 2010
Received in revised form 23 October 2010
Accepted 15 November 2010

Keywords:
Enrofloxacin
Antibacterial activity
DNA interaction
Salt effect
IC_{50}

ABSTRACT

Novel metal complexes of the second-generation quinolone antibacterial agent enrofloxacin with copper(II) and neutral bidentate ligands have been prepared and characterized with elemental analysis reflectance, IR and mass spectroscopy. Complexes have been screened for their *in-vitro* antibacterial activity against two Gram$^{(+ve)}$ *Staphylococcus aureus*, *Bacillus subtilis*, and three Gram$^{(-ve)}$ *Serratia marcescens*, *Escherichia coli* and *Pseudomonas aeruginosa* organisms using the double dilution technique. The binding of this complex with CT-DNA has been investigated by absorption titration, salt effect and viscosity measurements. Binding constant is ranging from 1.3×10^4–3.7×10^4. The cleavage ability of complexes has been assessed by gel electrophoresis using pUC19 DNA. The catalytic activity of the copper(II) complexes towards the superoxide anion ($O_2^{\bullet -}$) dismutation was assayed by their ability to inhibit the reduction of nitroblue tetrazolium (NBT).

1. Introduction

Fluoroquinolones suppress cell growth by inhibiting activity of DNA gyrase, an essential bacterial enzyme that maintains superhelical twists in DNA [1]. The detailed mechanism of the biological action of the compounds is not completely understood at present, and many different explanations of the activity of fluoroquinolones have been proposed. Some evidence suggests that the drugs interact directly with DNA, blocking the activity of DNA-gyrase repair enzymes [2,3].

Enrofloxacin is a typical second-generation antimicrobial drug with a broad spectrum of activity against a wide range of Gram-negative and Gram-positive bacteria, including those resistant to β-lactam antibiotics and sulfonamides. Enrofloxacin is the first fluoroquinolone developed for veterinary application and is potentially available for the treatment of urinary tract, respiratory tract and skin infectious diseases in pets and livestock [4]. The knowledge of structure of DNA and its interactions with other biological compounds can lead to advance in pharmacology and diagnosis basis of many diseases [5,6]. Sigman et al. [7] discovered in 1979 that complexes of copper(II) with 1,10-phenanthroline were capable of cleaving DNA. Copper complexes with a nitrogen donor heterocyclic ligand have been widely used to improve nuclease activity [8], mostly because of their high nucleolytic efficiency to break the DNA chain in the presence of H_2O_2 and reducing agents [9].

In recent years, the study of quinolones-copper-1,10-phenanthroline complexes becomes an increasingly important field due to antibacterial properties of the compounds [10]. In recent years, particular interest has been paid to synthetic analogs of CuZn-SOD [11]. In this perspective, the coordination and redox potentials of each Cu(II) ion in the synthesized copper(II) complexes which can be considered to possess SOD-mimic activity were found to play a significant role [12]. The central biological role of phosphate esters as constituents of nucleic acid chains has prompted the development of drugs able to cleave this class of compounds with a view to future application in biotechnology and medicine, to permit gene manipulation, and eventually novel therapeutic agents [13–15].

Herein, we represent the interaction of Cu(II) with the second-generation quinolone enrofloxacin and bidentate ligands and an attempt to examine the mode of coordination and biological properties of resultant complexes.

2. Experiments

2.1. Materials

All the chemicals for the synthesis of the compounds were used as purchased. Enrofloxacin was purchased from Bayer AG (Wuppertal, Germany). Cupric chloride was purchased from E. Merck (India) Ltd. Mumbai. 1,10-Phenanthroline and Luria Broth were purchased

* Corresponding author. Tel.: +91 2692 226856x202.
E-mail address: jeenen@gmail.com (M.N. Patel).

1386-1425/$ – see front matter © 2010 Elsevier B.V. All rights reserved.
doi:10.1016/j.saa.2010.11.056

from Himedia, India. 2,9-Dimethyl-1,10-phenanthroline (A^4) and 2,9-dimethyl-4,7-diphenyl-1,10-phenanthroline (A^5) were purchased from Loba chemie PVT. LTD. (India). Organic solvents were purified by standard method.

2.2. Instrumentation

Infrared spectra were measured in the 4000–400 cm^{-1} range on FT-IR Shimadzu spectrophotometer using KBr pellets. C, H and N elemental analyses were performed on a model Perkin Elmer 240 elemental analyzer. The metal contents of the complexes were analyzed by EDTA titration [16] after decomposing the organic matter with a mixture of $HClO_4$, H_2SO_4, and HNO_3 (1:1.5:2.5). The UV–Vis–near IR absorption spectra were recorded with a Perkin-Elmer Lambda-9 spectrophotometer, using the reflectance technique. Magnetic susceptibilities were measured on a Faraday magnetometer balance using $Hg[Co(SCN)_4]$ as a standard($\chi_g = 16.44 \times 10^{-6}$ cgs unit at 20 °C), and diamagnetic corrections were made by Pascal's constants [17]. The FAB mass spectra were recorded on a Jeol SX 120/Da-600 mass spectrometer/Data system using Argon/Xenon(6 kV, 10 mA) as FAB gas. The accelerating voltage was 10 kV and spectra were recorded at room temperature.

2.3. Ligand preparation

1,10-Phenanthroline-5,6-dione (A^2), 5-bromo-1,10-phenentroline(A^4) and 5-nitro-1,10-phenanthroline (A^5) were prepared as per the reported method [18–20].

2.4. Preparation of complexes

2.4.1. [Cu(erx)(A^1)Cl]

A methanolic solution of $CuCl_2{\cdot}2H_2O$ (1.5 mmol) was added to methanolic solution of 2,9-dimethyl-1,10-phenantroline (1.5 mmol), followed by the addition of a previously prepared solution of enrofloxacin (1.5 mmol) in methanol in the presence of CH_3ONa (1.5 mmol). The pH was adjusted at ~6.8 using dilute solution of CH_3ONa. The resulting solution was refluxed for 2 h on a water bath, followed by concentrating it to half of its volume. A fine green colored amorphous product obtained which was washed with ether/hexane and dried in vacuum desiccators (Scheme 1).

Yield: 65.7%, m.p.: 220 °C, μ_{eff}: 1.79 B.M. λ_{max}, 283 nm. ε, 87,888 L mol^{-1} cm^{-1}; λ_{max}, 318 nm. ε, 42,857 mol^{-1} cm^{-1}. Anal. Calc. for: $C_{33}H_{33}ClCuFN_5O_3$ (665.64): C, 59.54; H, 5.00; N, 10.52; Cu, 9.55%. Found: C, 59.46; H, 4.92; N, 10.48; Cu, 9.60.

In similar way, complexes 2–5 were prepared with the use of corresponding ligands.

2.4.2. [Cu(erx)(A^2)Cl]

It was prepared using 1,10-phenantroline-5,6-dione (1.5 mmol). Yield: 66.8%, m.p.: 207 °C, μ_{eff}:1.82 B.M. λ_{max}, 284 nm. ε, 77,148 L mol^{-1} cm^{-1}; λ_{max}, 318 nm. ε, 41,237 L mol^{-1} cm^{-1}. Anal. Calc. for: $C_{31}H_{27}ClCuFN_2O_5$ (667.57): C, 55.77; H, 4.08; N, 10.49; Cu, 9.52. Found: C, 55.71; H, 4.17; N, 10.45; Cu, 9.49%.

2.4.3. [Cu(erx)(A^3)Cl]

It was prepared using 2,9-dimethyl-4,7-diphenyl-1,10-phenantroline (1.5 mmol). Yield: 67.8%, m.p.: 182 °C, μ_{eff}:1.88 B.M. λ_{max}, 283 nm. ε, 76,211 L mol^{-1} cm^{-1}; λ_{max}, 319 nm. ε, 41,053 L mol^{-1} cm^{-1}. Anal. Calc. for: $C_{45}H_{41}ClCuFN_5O_3$ (817.59): C, 66.09; H, 5.05; N, 8.56; Cu, 7.77. Found: C, 66.02; H, 5.08; N, 8.51; Cu, 7.71%.

2.4.4. [Cu(erx)(A^4)Cl]

It was prepared using 5-bromo-1,10-phenantroline (1.5 mmol). Yield: 69.8%, m.p.: 186 °C, μ_{eff}:1.84 B.M. λ_{max}, 281 nm. ε, 71,739 L mol^{-1} cm^{-1}; λ_{max}, 314 nm. ε, 35,714 L mol^{-1} cm^{-1}. Anal. Calc. for: $C_{31}H_{28}BrClFCuN_5O_3$ (716.49): C, 51.97; H, 3.94; N, 9.77; Cu, 8.87. Found: C, 52.06; H, 3.99; N, 9.75; Cu, 8.98%.

2.4.5. [Cu(erx)(A^5)Cl]

It was prepared using 5-nitro-1,10-phenantroline (1.5 mmol). Yield: 67.8%, m.p.: 185 °C, μ_{eff}:1.87 B.M. λ_{max}, 281 nm. ε, 69,255 L mol^{-1} cm^{-1}; λ_{max}, 313 nm. ε, 34,161 L mol^{-1} cm^{-1}. Anal. Calc. for: $C_{31}H_{28}ClCuFN_6O_5$ (682.59): C, 54.55; H, 4.13; N, 11.72; Cu, 9.31. Found: C, 54.49; H, 4.06; N, 11.79; Cu, 9.23%.

2.5. Minimum inhibitory concentration

The antibacterial activity of the compounds (ligands, metal salts and complexes) was screened against two $Gram^{(+ve)}$ *Staphylococcus aureus*, *Bacillus subtilis*, and three $Gram^{(-ve)}$ *Serratia marcescens*, *Escherichia coli* and *Pseudomonas aeruginosa organisms*. Screening was performed by determining the minimum inhibitory concentration (MIC). Two different media [2% Luria Broth medium] were prepared. All cultures were incubated at 37 °C. Control tests with no active ingredients were also performed. The MIC was determined using twofold serial dilutions in liquid media of the compound being tested. The solvent used was DMSO.

A preculture of bacteria was grown in LB (Luria Broth) overnight at optimal temperature of each species. This culture was used as a control to examine if growth of the bacteria tested is normal. In a similar second culture, 20 μL of the bacteria as well as the tested compound at desired concentration was added. We monitored bacterial growth by measuring turbidity of the culture after 18 h. If a certain concentration of a compound inhibited bacterial growth, half the concentration of compound was tested. This procedure was carried on to a concentration that bacteria grow normally. The lowest concentration that inhibited bacterial growth was determined as MIC value. All equipment and culture media were sterile.

2.6. DNA interaction activity

2.6.1. Viscosity measurements

Viscometric studies were done using the Ubbelohde viscometer that was thermostated at 27 ± 0.1 °C in a constant temperature bath. DNA samples approximately 200 bp in length were prepared by sonicating in order to minimize complexities arising from DNA flexibility [21].

The concentration of DNA was 100 μM in NP and the flow times were measured with an automated timer. Each sample was measured 3 times. The rate of flow of sodium phosphate buffer (pH~7.2), DNA (100 μM) and DNA with the copper complexes at various concentrations were measured. The data were presented as $(\eta/\eta_0)^{1/3}$ versus [complex]/[DNA] [22], where η is the viscosity of DNA in the presence of complex and η_0 is viscosity of DNA in the absence of complex. Viscosity values were calculated from the flow time of DNA-containing solutions (t) corrected for that of buffer alone (t_0): $\eta = (t - t_0)$.

2.6.2. Absorption titration

A solution of CT DNA in 0.5 mM NaCl/5 mM Tris–HCl (pH 7.0) gave ratio of UV absorbance at 260 and 280 nm, A_{260}/A_{280} of 1.8–1.9, indicating DNA was sufficiently free of protein. So, no further effort was made to purify commercially obtained DNA. The concentration of DNA was determined by absorption spectroscopy using the ε value of 6600 mol^{-1} cm^{-1} L^{-1} at 260 nm [23]. The absorption titration of copper(II) complex in buffer (5 mM Tris–HCl, 50 mM NaCl, pH 7.0) was performed by using a fixed complex concentration to

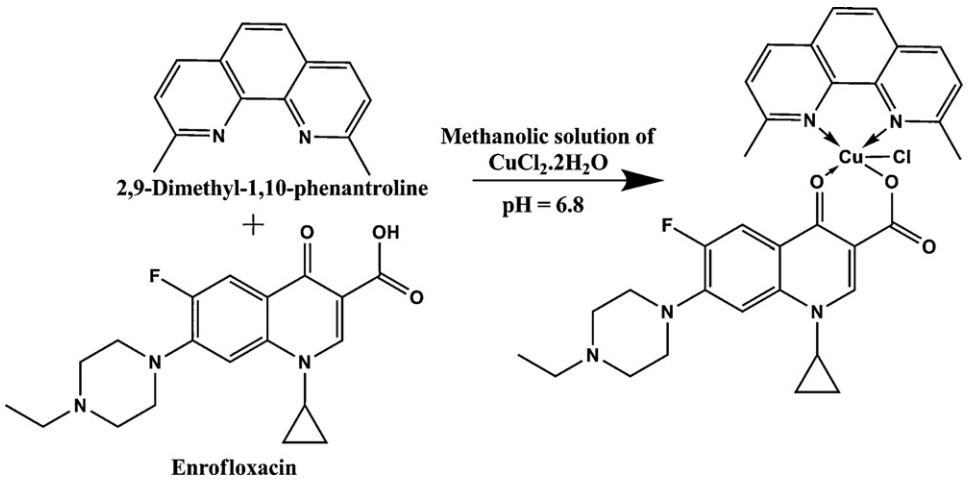

Scheme 1. Structure of the title complex $[Cu(erx)(A^1)Cl]\cdot 5H_2O$.

which increments of DNA stock solution were added. The concentration of copper(II) solution was 15 μM and DNA was added to a ratio of 6:1 [DNA]/[Cu]. Complex-DNA solutions were allowed to incubate for 5 min before the absorption spectra were recorded. The intrinsic binding constant K_b of copper(II) complex to DNA was calculated from Eq. (1) [24]

$$\frac{[DNA]}{\varepsilon_a - \varepsilon_f} = \frac{[DNA]}{\varepsilon_b - \varepsilon_f} + \frac{1}{k_b(\varepsilon_b - \varepsilon_f)} \quad (1)$$

where [DNA] is the concentration of CT-DNA in base pairs, the apparent absorption coefficients ε_a, ε_f, and ε_b correspond to A_{obsd}/[Cu], the absorbance for free copper complex, and the absorbance for copper complex in the fully bounded form, respectively. K_b is the equilibrium binding constant in M^{-1}.

2.6.3. Measurements of salt dependence in DNA binding

The equilibrium binding constant (K_b) of copper(II) complex to CT-DNA determined by spectrophotometric titration over the concentration range 0.005–0.100 M NaCl. A fixed amount of copper(II) complex in phosphate buffer at pH 7.2 and various concentrations of NaCl was titrated with increasing amounts of CT-DNA stock solutions (10^{-6}–10^{-4} M) and the hypochromicity in the μL at 281–284 nm. The K_b values at various NaCl concentrations were calculated on the basis of Eq. (1) [25–27].

The salt concentration dependence of K_b for the copper(II) complexes was evaluated by plotting $\log K_b$ versus $\log[Na^+]$ to obtain SK value, which is essential for polyelectrolyte analysis. Each measured point was the average value of at least three separate measurements with a relative standard deviation (RSD) normally less than 15%.

2.6.4. DNA cleavage study

Gel electrophoresis of plasmid DNA (pUC19 DNA) was carried out in TAE buffer (0.04 M Tris–Acetate, pH 8, 0.001 M EDTA). 15 μL reaction mixture containing plasmid DNA in TE buffer (10 mM Tris, 1 mM EDTA, pH 8.0) and 200 μM complex. Reactions were allowed to proceed for 3 h at 37 °C. All reactions were quenched by the addition of 5 μL loading buffer (0.25% bromophenol blue, 40% sucrose, 0.25% xylene cyanole, and 200 mM EDTA). The aliquots were loaded directly on to 1% agarose gel and electrophoresed at 50 V in 1X TAE buffer. Gel was stained with 0.5 μg/mL ethidium bromide and was photographed on a UV illuminator. The percentage of each form of DNA was quantities using AlphaDigiDoc™ RT. Version V.4.0.0 PC-Image software. For mechanistic investigations, experiments were carried out in the presence of radical scavenging agents, viz., DMSO ($OH^\bullet$ radical) and NaN_3 ($^1O_2$ radical) which were added to SC DNA prior to the addition of the complex.

2.7. Determination of SOD-like activity

SOD-like activity of all the complexes was determined by NBT/NADH/PMS system [28]. The superoxide radial produce by 79 μM NADH, 30 μM PMS, system containing 75 μM NBT, phosphate buffer (pH = 7.8), and 0.25–3.0 μM tested compound. The amount of reduced NBT was spectrophotometrically detected by monitoring the concentration of blue formazan form which absorbs at 560 nm. The reduction rate of NBT was measured in the presence and absence of test compounds at various concentration of complex in the system. All measurements were carried out at room temperature. IC_{50} value of all the complexes was determined by plotting graph of percentage inhibition of NBT reduction against increase in concentration of the complex. Concentration of the complex which causes 50% inhibition of NBT reduction is reported as IC_{50}.

3. Result and discussion

3.1. Characterization of complexes

All the complexes were analyzed using elemental analysis, magnetic measurements, reflectance, IR, FAB-mass spectroscopy. The elemental analysis is in concurrence with proposed 1:1:1, metal:erx:A^n formulation and theoretical expectation.

3.2. IR spectra

In Table 1 the characteristic absorptions of the IR spectra of the complexes are listed. In the IR spectra of complexes 1–5, the absorption at 1733 cm^{-1} in the spectrum of enrofloxacin attributed to the absorption of $\nu(C{=}O)_{carb}$ has disappeared. Two very strong characteristic bands are present in the range 1560–1675 cm^{-1} and 1345–1380 cm^{-1} that could be assigned as $\nu(COO)$ asymmetric and symmetric stretching vibrations, respectively, whereas $\nu(C{=}O)_p$ is shifted from 1615–1635 cm^{-1} upon bonding. The Δ values ($\Delta = \nu(COO)_{as} - \nu(COO)_s$, a useful characteristic for determining the coordination mode of ligands) fall in the range 197–214 cm^{-1} indicating a monodentate coordination mode of the carboxylato group of enrofloxacinato ligand [29].

These changes in the IR spectra suggest that enrofloxacin is coordinated to metal via pyridone and one carboxylate oxygen atoms [30]. These data are further supported by $\nu(M{-}O)$ [31] which appear

Table 1
IR spectra data.

Compounds	$\nu(C{=}O)_p$ (cm^{-1})	$\nu(COO)_{asy}$ (cm^{-1})	$\nu(COO)_{sym}$ (cm^{-1})	$\Delta\nu$ (cm^{-1})	ν(M–N) (cm^{-1})	ν(M–O) (cm^{-1})
Enrofloxacin	1622	1733	–	–	–	–
[Cu(erx)(A^1)Cl]	1634	1570	1369	201	538	510
[Cu(erx)(A^2)Cl]	1623	1575	1378	197	539	508
[Cu(erx)(A^3)Cl]	1622	1575	1373	202	542	513
[Cu(erx)(A^4)Cl]	1616	1570	1370	200	540	512
[Cu(erx)(A^5)Cl]	1620	1562	1348	214	542	511

at ~512 cm^{-1}. In investigated complexes, ν(C=N) band of ligands appears at 1580 cm^{-1}. N → M bonding was supported by ν(M–N) band [32] at ~535 cm^{-1}.

3.3. Reflectance spectra and magnetic behaviour

The reflectance spectra of Cu(II) complexes exhibit one asymmetric broad band centred around 15,000 cm^{-1}. These spectra suggest that compounds have a distorted square-pyramidal geometry arrangement [33].

The magnetic moments of the copper(II) complexes lie in the 1.79–1.88 BM range. These values are typical of mononuclear copper(II) compounds with d^9 electronic configuration. The observed magnetic moments of all the complexes correspond to typical high-spin distorted square-pyramidal complexes. However, the values are slightly higher than the expected spin-only values due to spin–orbit-coupling contribution [34].

3.4. FAB-mass

Fig. 1 represents the FAB-mass spectrum of complex 1, that is [Cu(erx)(A^1)Cl], obtained using *m*-nitro benzyl alcohol as matrix. Peaks at 136, 137, 154, 289 and 306 *m*/*z* are due to usage of matrix. The molecular ion peak is observed at *m*/*z* = 664 which is similar to the molecular weight of complex. Loss of chlorine atom gave a fragment ion peak at *m*/*z* = 630, which confirm that chlorine atom attached to metal ion with covalent bond. Fig. 1 shows the fragments corresponding to peaks at 456, 421, 359, 271 and 208 *m*/*z* value.

3.5. Antibacterial activity

Coordination compounds have been studied for their antitumour [35], antiviral [36] and antimalerial activity [37], which has been related to the ability of metal ions to form stable complexes [38]. The results have led to an understanding of coordination sphere and electronic properties of the metal ions and the factors such as chelate formation, ring size and number of chelate rings. Several workers have reported that heterocyclic rings containing sulfur, nitrogen, and/or oxygen are responsible for the biological activity of ligands and their metal complexes [39].

The antibactericidal activity of the cupric chloride, fluoroquinolones and its complexes were tested against two $Gram^{(+ve)}$ *S. aureus*, *B. subtilis*, and three $Gram^{(-ve)}$ *S. marcescens*, *E. coli* and *P. aeruginosa* organisms using double dilution method. An acceptable reason for this increase in bactericidal activity may be considered in the light of Overtone's concept [40] and chelation theory [41]. According to Overtone's concept of cell permeability, the lipid membrane that surrounds cell favors the passage of only lipid soluble materials so that liposolubility is an important factor which controls bactericidal activity. On chelation, the polarity of the cooper ion will be reduced to a greater extent due to the overlap of the ligand orbital and partial sharing of the positive charge of the copper ion with donor groups. Further, it increases the delocalization of π-electrons over whole chelate ring and enhances lipophilicity of the complexes. This increased lipophilicity enhances the penetration of the complexes into lipid membranes and blocks the metal binding sites in bacterial enzymes. These complexes also disturb the respiratory processes of the cell and thus block the synthesis of proteins which restricts further growth of the organism.

The results concerning in vitro antimicrobial activity (MIC) of ligands and their complexes are represented in Table 2. The antimicrobial activity of all complexes against five microorganisms is much higher than metal salt. The complex shows better antimicrobial activity than the metal salt, free ligands, and enrofloxacin. In case of *S. aureus*, all complexes have good activity compare to enrofloxacin. In case of *B. subtilis* complexes II–IV have good activity compare to standard drug. In case of *S. marcescens* and *E. coli* all complexes found more potent than enrofloxacin. In case of *P. aeruginosa* complexes I–III have good activity compare to standardized drug.

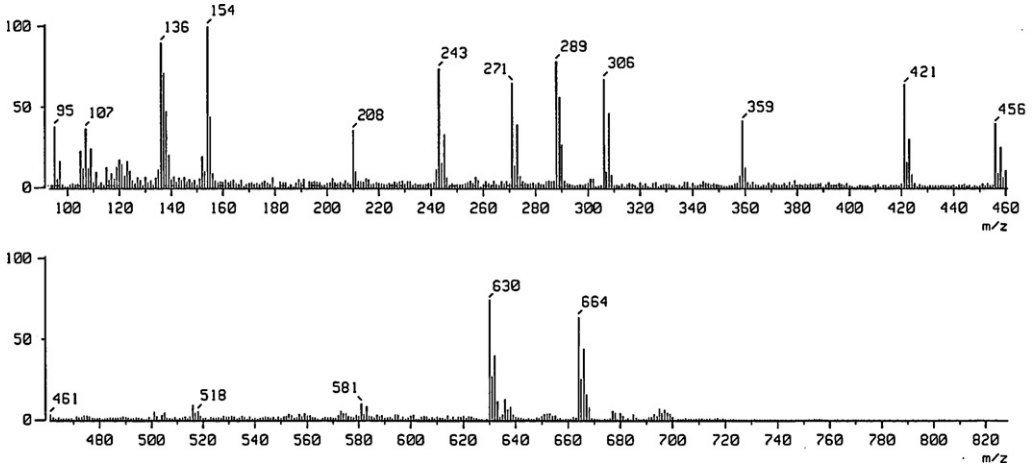

Fig. 1. FAB-mass spectrum of complex 1, that is [Cu(erx)(A^1)Cl], obtained using *m*-nitro benzyl alcohol.

Table 2
MIC data of the compounds (μM).

	S. aureus	*B. subtilis*	*S. marcescens*	*P. aeruginosa*	*E. coli*
$CuCl_2{\cdot}2H_2O$	2698.00	2815.00	2756.00	2404.00	3402.00
Ciprofloxacin	1.6	1.1	1.6	1.4	1.4
Gatifloxacin	5.1	4.0	2.9	1.0	2.9
Norfloxacin	2.5	2.5	4.1	3.8	2.8
Enrofloxacin	1.9	3.9	1.7	1.4	1.4
Pefloxacin	2.1	2.4	5.1	5.7	2.7
Levofloxacin	1.7	2.2	1.7	1.7	1.0
Sparfloxacin	1.3	2.0	1.5	1.5	1.3
Ofloxacin	1.9	1.4	1.7	2.2	1.4
[Cu(erx)(A^1)Cl]	0.45	1.94	0.6	1.06	0.6
[Cu(erx)(A^2)Cl]	0.74	1.39	0.44	1.19	1.19
[Cu(erx)(A^3)Cl]	0.36	1.1	0.48	0.8	0.48
[Cu(erx)(A^4)Cl]	1.05	1.11	1.53	1.67	1.25
[Cu(erx)(A^5)Cl]	0.58	2.07	0.58	1.61	1.02

It was observed that all complexes were more bacteriostatic than ligands. When antimicrobial activity of metal complexes is investigated, the following principal factors [42] should be considered: (i) the chelate effect of the ligands; (ii) the nature of the N-donor ligands; (iii) the total charge of the complex; (iv) the existence and the nature of the ion neutralizing the ionic complex; (v) the nuclearity of the metal centre in the complex.

The first two of the five above-mentioned factors may be responsible for higher antimicrobial activity; that is the chelate effect provided by both the enrofloxacin ligand and the N-donor ligand and the nature of the ligands.

This is probably one of the main reasons for the diverse antibacterial activities shown by the complexes. The significant improvement of the activity of enrofloxacin when coordinated to the copper complex is simply an evidence of the role of the coordinated metal ion.

3.6. Complex-DNA interaction

3.6.1. Absorption titration

Complex binding with CT-DNA through intercalation usually result in hypochromism and bathochromism, due to intercalative mode involving a strong stacking interaction between an aromatic chromophore and the base pairs of DNA [43,44].

The binding of Cu(II) complexes to duplex DNA led to decrease in the absorption intensities with a small amount of red shifts in the UV–Vis absorption spectra. After intercalating the base pairs of DNA, the π^* orbital of the intercalated ligand can couple with the π orbital of base pairs, thus decreasing the π–π^* transition energy and resulting in the bathochromism [45,46].

On the other hand, the coupling π orbital is partially filled by electrons, thus decreasing the transition probabilities and concomitantly resulting in hypochromism. The binding constant (K_b) of the complexes to DNA were determined by monitoring the changes of absorbance at 281–284 nm with increasing concentration of DNA (Fig. 2). The appreciable decrease in absorption intensity and significant red shift of the π–π^* band of complexes is similar to that observed for its interaction with DNA in DMSO solution, suggesting that the complex bind to DNA strongly. The binding constant (K_b) of complexes (Table 3) are in the range of 1.3×10^4–3.7×10^4.

Table 3
Binding constants (K_b) and IC_{50} value of the complexes.

Complexes	K_b (M^{-1})	IC_{50}
[Cu(erx)(A^1)Cl]	1.31×10^4	0.875
[Cu(erx)(A^2)Cl]	3.63×10^4	1.45
[Cu(erx)(A^3)Cl]	1.57×10^4	0.5
[Cu(erx)(A^4)Cl]	1.65×10^4	1.25
[Cu(erx)(A^5)Cl]	1.61×10^4	0.8

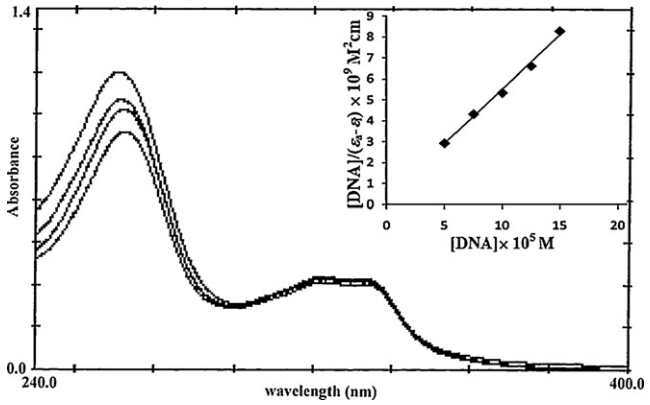

Fig. 2. Absorption titration curve of [Cu(erx)(A^1)Cl] in absence and presence of increasing amount of DNA; 50–150 μM in phosphate buffer(Na_2HPO_4/NaH_2PO_4, pH 7.2), [complex] = 15 μM at 281–284 nm, with incubation period of 30 min at 37 °C, Inset: plot of [DNA]/($\varepsilon_a - \varepsilon_f$) versus [DNA].

Comparing the intrinsic binding constant of complexes with those of DNA-intercalative $[Ru(dmb)_2(ipbp)]^{+2}$ ($1.18 \times 10^4\ M^{-1}$) complex [47], we can deduce that all the complex bind strongly to DNA by intercalation. These spectral characteristics obviously suggest that complexes interact with DNA most likely through a mode that involves a stacking interaction between the aromatic chromophore and the base pairs of DNA.

3.6.2. Viscosity measurement

Binding modes of the complexes were further investigated by viscosity measurements. Though photophysical experiments, give necessary information about binding modes of metal complexes with DNA, they do not provide conclusive evidences for the exact mode of binding. Hydrodynamic measurements such as viscosity which is sensitive to length changes are regarded as the least uncertain and the most critical tests of binding modes in solution [48]. Viscosity of DNA is increased in the case of classical intercalator due to increase in the length of DNA helix, as base pairs are separated to accommodate the intercalator.

There are many cases in which complexes having square pyramidal geometry and shows classical intercalation [49–51]. The binding of DNA with complexes depends upon nature of ligands. In present study, the bidentate ligands which have different substituent's and intercalation in nature. Spectral characteristics are consistent with a mode of interaction that involves a stacking interaction between the complex and the base pairs of DNA, which means that the complexes can intercalate into the double helix structure of DNA.

From Fig. 3, as increasing the amounts of complexes, the viscosity of DNA increases steadily, which is similar to that of the classical intercalative complex $[Ru(dmb)_2(ipbp)]^{+2}$ [47]. The binding ability of complexes is more compare to enrofloxacin and less compare to classical intercalator ethidium bromide. Among all complexes, complexes 2, 3 and 5 bind more strongly than 1 and 5.

3.6.3. Salt effect

The overturn salt titration is an efficient method to discriminate binding modes between the bound molecules and DNA. The detailed results are collected in Table 4. The binding constants for all the complexes reported were obtained over the concentration range 0.005–0.100 M NaCl in order to apply polyelectrolyte theory to the calculation of the non-electrostatic binding constants and separate the binding free energy change into its electrostatic and non-electrostatic contributions. The salt concentrations of 0.005–0.100 M were selected in this study because the polyelectrolyte theories which will be used for successive analysis are based

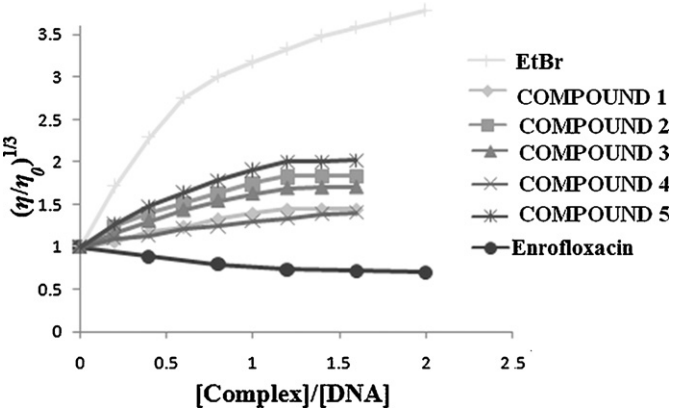

Fig. 3. Effect on relative viscosity of DNA under the influence of increasing amount of complexes at 27 ± 0.1 °C in phosphate buffer.

Table 4
Equilibrium binding constant (K_b) for the binding of complex-I to DNA.

[NaCl] (M)	K_b (M^{-1} bp) × 10^4	K_t^0 (M^{-1} bp) × 10^4	K_t^0/K_b (%)
0.005	3.367	0.3626	10.96
0.025	2.020	0.4158	20.58
0.050	1.662	0.4438	26.67
0.075	1.273	0.3991	31.35
0.100	0.9233	0.3278	35.5

Average: 0.389 × 10^4

on limiting laws that are exactingly applicable to salt concentrations of lower than 0.100 M [52].

The plot of log[Na^+] against log K_b for the binding of copper(II) complexes to CT-DNA is given in Fig. 4. It is clear from the plots that the binding constant decreases with increasing salt concentration. Using the slope of Fig. 4, we calculated non-electrostatic binding constant (K_t^0) at various concentrations of NaCl ([M^+]) using Eq. (2):

$$\ln K_b = \ln K_t^0 + Z\xi^{-1}\{\ln(\gamma \pm \delta)\} + Z\psi(\ln[M^+]) \quad (2)$$

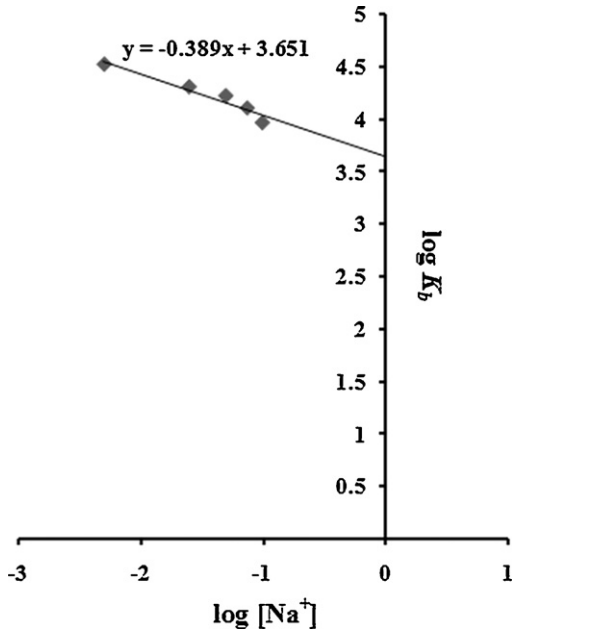

Fig. 4. The dependence of the DNA binding constant of the Cu(II) complex on the salt concentrations.

where $Z\psi$ is estimated from the slope of the decay line in Fig. 4. Z is partial charge on the binding ligand involved in the DNA interaction, ψ is the fraction of counterions coupled with each DNA phosphate (ψ = 0.88 for double-stranded B-form DNA), $\gamma_\pm$ is the mean activity coefficient at cation concentration M^+, and the remaining terms are constants for double stranded DNA in B-form, i.e. ξ = 4.2 and δ = 0.56. Results of calculations are summarized in Table 4 along with percentage of K_t^0 contribution to the total binding constants (K_b) at various concentrations of Na^+. These K_t^0 can be taken as measure large non-electrostatic forces stabilize the ligand–DNA interaction. In contrast to the K_b values which are salt-dependent, the magnitude of K_t^0 is constant throughout the concentration of NaCl employed with the average value of 3.89×10^4 M^{-1} bp (RSD = 12.5%). Although the values of K_t^0 are constant throughout the concentrations of salt, the percentage of K_t^0 contributions to the K_b increases significantly and reach a maximum of 35.5% at [Na^+] = 0.1 M. It can be expected that at higher concentrations of salt.

Analysis is also possible to dissect the binding free energy change (ΔG^0) for the binding of copper(II) to CT-DNA into its electrostatic ($\Delta G_{pe}{}^0$) and non-electrostatic ($\Delta G_t{}^0$) contributions at a given concentration of NaCl. Table 5 summarizes the results of energetics calculation for the binding of Cu(II) to CT-DNA in 0.050 M NaCl along with those of other copper(II) complexes [53,54] for the purpose of comparison. The total binding free energy changes listed in Table 5 were calculated based on the standard Gibbs relation.

The observed binding constant K_b is a function of the charge on the cation (Z), the fraction of counter ion associated with each DNA phosphate (ψ) which is generally taken to be 0.88 for double-stranded B-form DNA. A slope in a plot of log K_b versus log[Na^+] is equal to SK in Eq. (3):

$$SK = \frac{\delta \log K_b}{\delta \log[Na^+]} = -Z\psi \quad (3)$$

$$\Delta G^0 = -RT \ln K_b \quad (4)$$

$$\Delta G_{pe}^0 = SKRT \ln[Na^+] \quad (5)$$

$$\Delta G_t^0 = \Delta G^0 - \Delta G_{pe}^0 \quad (6)$$

The binding free energy can be calculated from Eq. (4). Electrostatic (ΔG_{pe}^0) and nonelectrostatic (ΔG_t^0) of the free energy can be calculated from Eqs. (5) and (6), respectively. A nonelectrostatic free energy ΔG_t^0 was derived to be −20.4 kJ mol^{-1}, and electrostatic free energy ΔG_{pe}^0 of −6.3 kJ mol^{-1} in 50 mM NaCl. It is apparent that electrostatic contribution to the free energy is much less than nonelectrostatic portion, strongly supporting theory that the terpyridine moiety is intercalated between base pairs of the DNA helix [55].

The result of quantitative analysis suggests that the main contribution to the stabilization of DNA binding comes from nonelectrostatic interaction as indicated by their $\Delta G_t{}^0$ values is at 87% relative to the total binding free energy change.

3.6.4. Gel electrophoresis

Cleavage of plasmid pUC19 DNA by synthesized complexes was monitored by agarose gel electrophoresis technique. When plasmid DNA was subjected to electrophoresis after interaction, upon illumination of gel (Fig. 5) the fastest migration was observed for super coiled (SC) Form I, where as the slowest moving was open circular (OC) Form II and the intermediate moving is the linear (NC) Form III generated on cleavage of open circular. The data of plasmid cleavage are presented in Table 6. All the complexes show higher DNA cleavage ability compare to the drug and metal salt. Complexes 1–5 do not show inhibition of DNA cleavage in the presence of scavengers of hydroxyl radicals (DMSO) (Supply 1) and singlet oxygen (sodium azide) (Supply 2). This indicates that the cleavage of DNA probably

Table 5
Thermodynamic parameter for the binding of copper(II) complexes to CT-DNA.

Binding ligand	K_b (10^4 M^{-1} bp)	ΔG^0	*SK*	ΔG^0_{pe}	$K_t^0/10^3$ (%K_t^0/K_b) M^{-1} bp)	ΔG_t^0 (%$\Delta G_t^0/\Delta Go$)
[Cu(erx)(A^1)Cl]	1.662	−240.37	0.389	−28.82	3.626(26.67)	−211.55 (88.01)
[Cu(erx)(A^2)Cl]	1.522	−239.19	0.385	−28.52	4.196(27.56)	−210.67 (88.07)
[Cu(erx)(A^3)Cl]	1.680	−240.64	0.415	−30.75	4.119(24.51)	−209.89 (87.22)
[Cu(erx)(A^4)Cl]	1.544	−238.55	0.372	−27.63	4.394(28.45)	−210.92 (88.41)
[Cu(erx)(A^5)Cl]	1.589	−239.26	0.376	−27.86	4.460(28.06)	*−211.40 (88.35)*

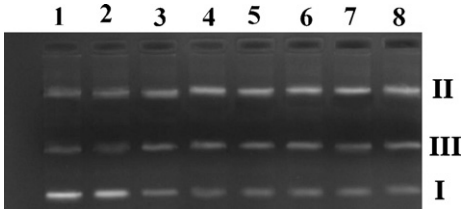

Fig. 5. Photogenic view of interaction of pUC19 DNA (300 μg/mL) with of copper(II) complexes (200 μM) using 1% agarose gel containing 0.5 μg/mL ethidium bromide. All reactions were incubated in TE buffer (pH 8) in a final volume of 15 μL, for 3h. at 37 °C. Lane 1, DNA control; Lane 2, $CuCl_2{\cdot}2H_2O$; Lane 3, enrofloxacin; Lane 4, [Cu(erx)(A^1)Cl]; Lane 5, [Cu(erx)(A^2)Cl]; Lane 6, [Cu(erx)(A^3)Cl]; Lane 7, [Cu(erx)(A^4)Cl]; Lane 8, [Cu(erx)(A^5)Cl].

Table 6
Gel electrophoresis data.

Compounds	% SC	% OC	% LC	% Cleavage
DNA control	68	14	18	–
DNA + Metal salt	57	17	26	16.17
DNA + Enrofloxacin	35	24	41	48.52
DNA + I	19	34	47	72.05
DNA + II	23	31	46	66.17
DNA + III	22	32	46	67.67
DNA + IV	26	26	48	61.76
DNA + V	21	31	48	69.11

follows a hydrolytic cleavage mechanism. Such DNA hydrolysis by copper(II) complexes have been reported earlier [56].

3.7. SOD mimic activity

The system used as a basis of superoxide radical generator in order to check SOD like activity of the synthesized complexes was NBT/NADH/PMS system. Absorbance at a function of time was plotted to have a straight line obeying equation $Y = mX + C$ (Fig. 6).

Fig. 7 shows percentage inhibition of reduction of nitro blue tetrazolium (NBT) plotted against concentration of the complex-

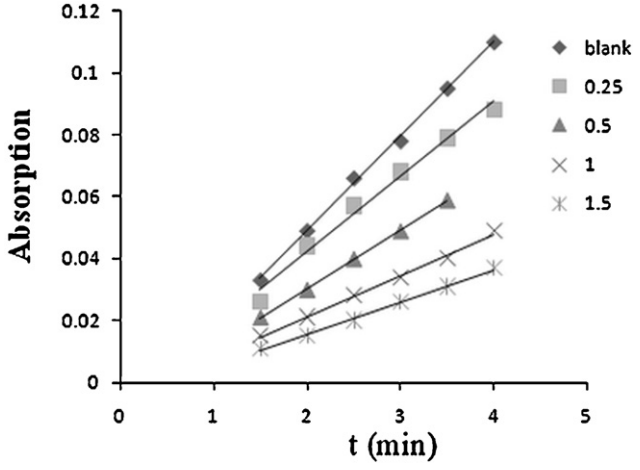

Fig. 6. Plot of absorbance values(Abs_{560}) against time (t).

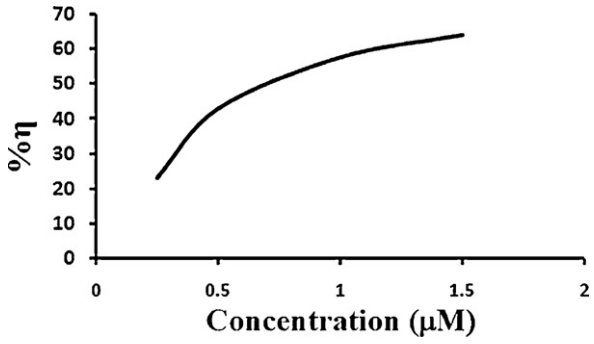

Fig. 7. Plot of percentage of inhibiting NBT reduction with an increase in the concentration of complex 1.

1. Compounds exhibit SOD-like activity at biological pH with their IC_{50} values ranging from 0.5 to 1.45 μM. The superoxide scavenging data are presented in Table 3. The higher IC_{50} can only be accredited to the vacant coordination site facilitating the binding of superoxide anion, electrons of aromatic ligands that stabilize $Cu–O_2^{\bullet-}$ interaction and not only to the partial dissociation of complex in solution.

Acknowledgements

Authors thank Head, Department of Chemistry, Sardar Patel University, India, for making it convenient to work in laboratory and U.G.C. for providing financial support under "UGC Research Fellowship in Science for Meritorious Students" scheme.

Appendix A. Supplementary data

Supplementary data associated with this article can be found, in the online version, at doi:10.1016/j.saa.2010.11.056.

References

[1] G. Klopman, S. Wang, M.R. Jacobs, S. Bajaksouzian, K. Edmonds, J.J. Ellner, Antimicrob. Agents Chemother. 37 (1993) 1799–1806.
[2] L. Shen, A.G. Pernet, Proc. Natl. Acad. Sci. U.S.A. 82 (1985) 307–311.
[3] L.L. Shen, in: D.C. Hopper, J.S. Wolfson (Eds.), Quinolone Antimicrobial Agents, 2nd ed., American Society for Microbiology, Washington, DC, 1993, p. p77.
[4] A. Tarushi, C.P. Raptopoulou, V. Psycharis, A. Terzis, G. Psomas, D.P. Kessissoglo, Bioorg. Med. Chem. 18 (2010) 2678–2685.
[5] K. Pinar, M. Burcu, Z. Aysin, O. Mehmet, Anal. Chim. Acta 518 (2004) 69–76.
[6] S. Pankaj, G.K. Werner, Anal. Chem. 69 (1997) 3552–3557.
[7] D.S. Sigman, D.R. Graham, V.D. Aurora, A.M. Stern, J. Biol. Chem. 254 (1979) 12269–12272.
[8] S.A. Ross, M. Pitie, B. Meunier, Eur. J. Inorg. Chem. 3 (1999) 557–563.
[9] L.Z. Li, C. Zhao, T. Xu, H. Ji, Y. Yu, G. Guo, H. Chao, J. Inorg. Biochem. 99 (2005) 1076–1082.
[10] J. Alos, Quinolones. Enferm. Infec. Microbiol. Clin. 21 (2003) 261–267.
[11] J. Casanova, G. Alzuet, J. Borrhs, J. Timoneda, S.G. Gradna, I.C. Gonzalex, J. Inorg. Biochem. 56 (1994) 65–76.
[12] D.M. Miller, G.R. Buttner, S.D. Aust, Biol. Med. 8 (1990) 95–108.
[13] L.M. Rossi, A. Neves, A.J. Bortoluzzi, R. Horner, B. Szpoganicz, H. Terenzi, A.S. Mangrich, E. Pereira-Maia, E.E. Castellano, W. Haase, Inorg. Chim. Acta 358 (2005) 1807–1822.
[14] M. Roy, S. Saha, A.K. Patra, M. Nethaji, A.R. Chakravarty, Inorg. Chem. 46 (2007) 4368–4370.
[15] M. Roy, T. Bhowmick, R. Santhanagopal, S. Ramakumar, A.R. Chakravarty, Dalton Trans. (2009) 4671–4682.

[16] A.I. Vogel, Textbook of Quantitative Inorganic Analysis, 4th ed., ELBS and Longman, London, 1978.
[17] P. Pascal, Compt. Rend. 57 (1944) 218.
[18] L.J. Henderson Jr., F.R. Fronczek, W.R. Cherry, J. Am. Chem. Soc. 106 (1984) 5876–5879.
[19] C. Hiort, P. Lincoln, B. Norden, J. Am. Chem. Soc. 115 (1993) 3448–3454.
[20] G.F. Smith, Jr. Cagle, J. Org. Chem. 12 (1947) 781–784.
[21] J.B. Chaires, N. Dattagupta, D.M. Crothers, Biochemistry 21 (1982) 3933–3940.
[22] G. Cohen, H. Eisenberg, Biopolymer 8 (1969) 45–55.
[23] M.E. Reichmann, S.A. Rice, C.A. Thomas, P. Doty, J. Am. Chem. Soc. 76 (1954) 3047–3053.
[24] M.T. Carter, M. Rodriguez, A. Bard, J. Am. Chem. Soc. 111 (1989) 8901–8911.
[25] R.E. Holmlin, E.D.A. Stemp, J.K. Barton, Inorg. Chem. 37 (1998) 29–34.
[26] A.M. Pyle, J.P. Rehmann, R. Meshoyrer, C.V. Kumar, N.J. Turro, J.K. Barton, J. Am. Chem. Soc. 111 (1989) 3051–3058.
[27] S. Mahadevan, M. Palaniandavar, Inorg. Chem. 37 (1998) 693–700.
[28] V. Ponti, M.V. Dianzaini, K.J. Cheesoman, T.F. Stater, Chem. Biol. Interact. 23 (1978) 281–291.
[29] K. Nakamoto, Infrared and Raman Spectra of Inorganic and Coordination Compounds, 4th ed., Wiley, New York, 1986.
[30] I. Turel, Coord. Chem. Rev. 232 (2002) 27–47.
[31] I. Turel, I. Leban, N. Bukovec, J. Inorg. Biochem. 66 (1997) 241–247.
[32] H.H. Freedman, J. Am. Chem. Soc. 83 (1961) 2900–2905.
[33] A.B.P. Lever, Inorganic Electronic Spectroscopy, 2nd ed., Elsevier, Amsterdam, 1984.
[34] R. Carballo, A. Castineiras, B. Covelo, E. Garcia-Martinez, J. Niclos, E.M. Vazquez-Lopez, Polyhedron 23 (2004) 1505–1518.
[35] W.E. Anthroline, J.M. Knight, D.H. Petering, Inorg. Chem. 16 (1977) 569–574.
[36] D.H. Jones, R. Slack, S. Squires, K.R.H. Wooldrige, J. Med. Chem. 8 (1965) 676–680.
[37] D.L. Klayman, J.P. Sconill, J.F. Bafosevich, J. Bruce, J. Med. Chem. 26 (1983) 35–39.
[38] K.C. Agrawal, A.C. Santorelli, J. Med. Chem. 21 (1978) 218–221.
[39] R.C. Sharma, S.P. Trpathi, R.S. Sharma, Curr. Sci. 50 (1981) 748–750.
[40] Y. Anjaneyula, R.P. Rao, Synth. React. Inorg. Met. Org. Chem. 16 (1986) 257.
[41] P.K. Panchal, P.B. Pansuriya, M.N. Patel, J. Enzyme Inhib. Med. Chem. 21 (2006) 453–458.
[42] H.W. Rossmore, Disinfection, Sterilization and Preservation, 4th ed., Lea & Febiger, Philadelphia, 1991, pp. 290–321.
[43] B. Peng, H. Chao, B. Sun, H. Li, F. Gao, L.-N. Ji, J. Inorg. Biochem. 100 (2006) 1487–1494.
[44] P.U. Maheswari, M. Palaniandavar, J. Inorg. Biochem. 98 (2004) 219–230.
[45] V. Uma, M. Kanthimathi, T. Weyhermuller, B. Unni Nair, J. Inorg. Biochem. 99 (2005) 2299–2307.
[46] S. Ramakrishnan, M. Palaniandavar, J. Chem. Sci. 117 (2005) 179–186.
[47] Y.J. Liu, X.Y. Guan, X.Y. Wei, L.X. He, W.J. Mei, J.H. Yao, Transit. Met. Chem. 33 (2008) 289–294.
[48] G. Yang, J.Z. Wu, L. Wang, L.N. Ji, X. Tian, J. Inorg. Biochem. 66 (1997) 141–144.
[49] R. Rao, A.K. Patra, P.R. Chetana, Polyhedron 27 (2008) 1343–1352.
[50] P.R. Reddy, N. Raju, P. Manjula, K.V.G. Reddy, Chem. Biodivers. 4 (2007) 1565–1577.
[51] Y.-L. Song, Y.-T. Li, Z.-Y. Wu, J. Inorg. Biochem. 102 (2008) 1691–1699.
[52] I. Haq, P. Lincoln, D. Suh, B. Norden, B.Z. Chowdhry, J.B. Chaires, J. Am. Chem. Soc. 117 (1995) 4788–4796.
[53] S. Satyanarayana, J.C. Dabrowiak, J.B. Chaires, Biochemistry 31 (1992) 9319–9324.
[54] K. Mudasir, N. Wijaya, H. Yoshioka, J. Inorg. Biochem. 94 (2003) 263–271.
[55] Mudasir, K. Wijaya, E.T. Wahyuni, N. Yoshioka, H. Inoue, Biophys. Chem. 121 (2006) 44–50.
[56] A. Barve, A. Kumbhar, M. Bhat, B. Joshi, R. Butcher, U. Sonawane, R. Joshi, Inorg. Chem. 48 (2009) 9120–9132.